Proceedings in Manufacturing Systems, Volume 11, Issue 2, 2016, 89–94 ISSN 2067-9238

NUMERICAL AND EXPERIMENTAL ANALYSIS OF THE FORMABILITY OF 1.4301 AUSTENITIC STAINLESS STEEL SHEETS USING HYDROFORMING

Radu VASILE[1, *], Sever-Gabriel RACZ[2], Octavian BOLOGA[3]

[1)] Ph.D. Student, Department of Industrial Machinery and Equipment "Lucian Blaga" University, Sibiu, Romania
[2)] Prof. Ph.D., Head of Department, Department of Industrial Machinery and Equipment "Lucian Blaga" University, Sibiu, Romania
[3)] Prof. Ph.D., Department of Industrial Machinery and Equipment "Lucian Blaga" University, Sibiu, Romania

Abstract: *The present paper aims to analyse the forming capacity of stainless steel materials with hydroforming forming process. For this research, 1.4301 (X5CrNi18-10) austenitic stainless steel has been in focus for numerical and experimental analysis. The main advertised advantages of this material are ease of formability, good corrosion resistance and excellent aesthetic appearance for the end product. For proper forming evaluation tensile test, forming limit curves – Nakajima test have been carried out. The main material mechanical characteristics were processed in order to determine an accurate finite element model. The hydroforming drawn part was formed by a newly developed hydroforming press concept, developed by the authors. The numerical results were compared to the measured experimental results with the help of optical strain measurement software.*

Keywords: *numerical simulation, sheet metal forming, hydroforming, experimental research, stainless steel, CAD design, uniaxial tensile test, forming limit curve.*

1. INTRODUCTION

Hydroforming, an unconventional cold forming process, is used in manufacturing complex cave products from one operation. Fluid under pressure is used to form blank tubes and sheet metal. Hydroforming is also known as hydro-mechanical deep-drawing, stretch forming, activator assisted hydroforming etc. It is mostly used in automotive and aerospace industry for its great technical and economic potential, but also in less known fields like music industry and bicycle industry [1, 2].

Increasingly technologized times push companies to combine many technological fields in order to meet the increasing demands of the end-user. Only close connection between industry and research creates the necessary technological advance by bringing continuous innovation to products and technologies [3].

Products with high requirements and complex shapes transfer the complexity to the machines and therefore to the necessary tools. This complexity translates into costs that make unprofitable the conventional forming processes. People working in industry and research invest in developing new design methods for efficient and sustainable production to reduce costs [4].

Hydroforming shares the same materials used in conventional forming processes, such as alloyed and non-alloyed steels, titanium, copper and copper alloys &c.

Drucker Worldwide predicts significant changes in the material mix for body and closure parts. Materials like advanced high strength steels and aluminium have been increasingly used in the past years, mostly in the automotive industry.

As future predictions go use of advanced high strength steels will grow 77% in car body and closure parts by 2025 as represented in Fig. 1 [5].

Austenitic stainless steels show excellent forming performance during hydroforming due to higher hardening and elongation capacity. These material qualities delay defects during forming, but also require higher process forces [6].

Beginning from the previous statements the present paper aims to study and analyse the influence of die radius variation in hydroforming of 1.4301 austenitic stainless steel sheets. Evaluating the forming capacity by the main strains, thickness reduction and forming limits.

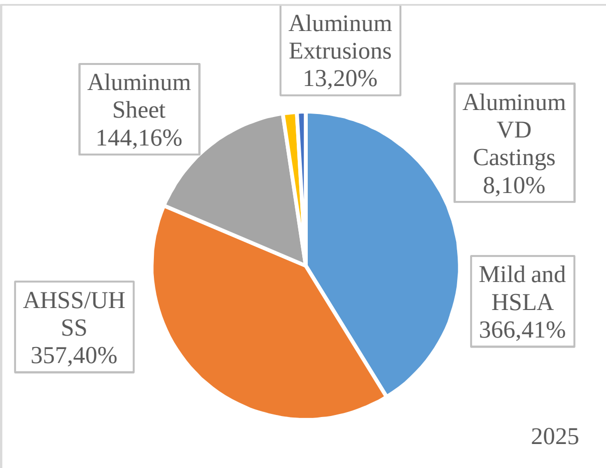

Fig. 1. Predictions on material use in car body and closure parts by 2025 [5].

* Corresponding author: "Lucian Blaga" University, Victoriei 10, 550024 Sibiu, Romania,
Tel.: +40 269 216062 ext 1450;
Fax: +40 269 217871;
E-mail addresses: *radu.vasile88@gmail.com* (R. Vasile), *gabriel.racz@ulbsibiu.ro* (G. Racz), *octavian.bologa@ulbsibiu.ro* (O Bologa).

Table 1

Chemical composition of 1.4301 stainless steel, content in [wt%] [7]

C	Si	Mn	P	S	Cr	Mo
0.02	0.32	1.45	0.031	0.035	17.85	0.42
Ni	**Al**	**Nb**	**Cu**	**Ti**	**V**	**Co**
8.470	0.008	0.007	0.299	0.005	0.092	0.180

2. MATERIALS USED IN THE RESEARCH

A representative stainless steel has been chosen for the experimental research, the austenitic 1.4301 (X5CrNi18-10) – EN 10088-3. Chromium-nickel austenitic stainless steel 1.4301 is the standard for the austenitic grades of stainless steel due to its good corrosion resistance, ease of formability and fabrication coupled with its aesthetic appearance in the polished, ground and brushed conditions.

The chemical composition of 1.4301 stainless steel is presented in Table 1 [7]. The physical and mechanical properties are presented in Table 2 [8, 9].

3. EXPERIMENTAL RESEARCH

The research directions are the following ones:

- Tensile test - determination of the mechanical parameters and the characteristic properties;
- Nakajima test with Hašek test samples- forming limit curves determination;
- Numerical analysis with finite element method in Abaqus software;
- Hydroforming process on new, custom built press by the authors;
- Strain measurement of the drawn parts with Argus software.

3.1. Uniaxial tensile test

The uniaxial tensile test was carried out using test samples made of 1.4301 austenitic stainless steel, of 1 mm thickness, at 0°, 45° and 90° compared to the blank rolling direction. The following experimental setup was carried out – a tensile testing machine Instron 5587 controlled by Blue-hill software from a PC and two CCD cameras connected to GOM PC with the optical strains measurement system Aramis (Fig. 3);

Table 2

Physical and mechanical properties of 1.4301 stainless steel [8, 9]

Properties at 20°C	Value EN 10088-2 [8]	Value [9]
Density ρ [kg/dm^3]	7.9	–
Young's Modulus E[GPa]	200	–
Yield Stress $R_{p0.2}$ [MPa]	190-235	315
Tensile Stress R_m [MPa]	500–700	708
Anisotropy r [-]	–	0.779
Poisson's Ratio ν [-]	0.3	–
Strain hardening exponent n [-]	–	0.441
Strength coefficient K [MPa]	–	1547

Fig. 3. Tensile test experimental configuration – GOM PC with Aramis software (left), Instron 5587 (centre), two CCD cameras (right front), PC with Blue-hill Software (right back).

With this experimental configuration the authors have determined the main mechanical characteristics of 1.4301. The test specimen has been designed according to ISO 6892-1:2009 [10]. With Instron testing machine and Aramis software yield stress, tensile strength, plastic strain, stain hardening exponent and strength coefficient for the test specimens have been determined.

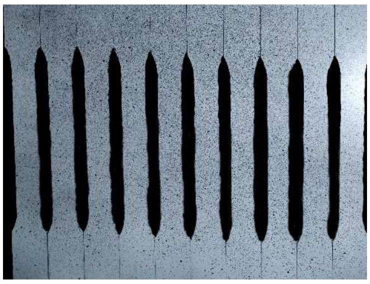

Fig. 4. Tensile test – test samples with a diffuse network of points applied (before the test).

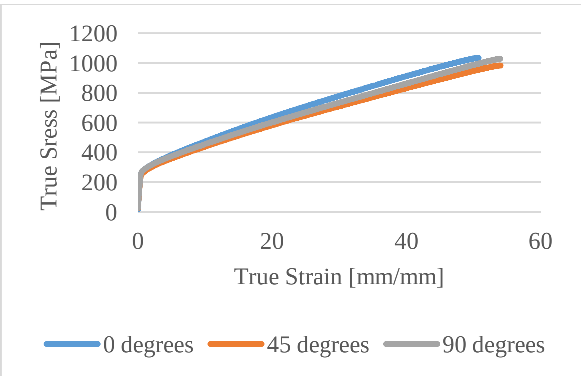

Fig. 5. The true strain-stress curve for 1.4301.

Results are represented in Table 3. With the GOM setup used as extensometer – based on a diffuse network of points applied on the test samples (Fig. 4), this optical system can measure the point's displacements during the tensile test process and thus it is possible to determine major and minor strains for the test specimen. Also with this setup the plane anisotropy coefficients were determined – r_{00}, r_{45} and r_{90} according to ISO 10113:2006 standard for the three degrees compared to the blank rolling direction [11]. Results are represented in Table 4. Fig. 5 represents the true stress – true strain curves obtained from the tensile tests, for the case in which the stretching occurred on three directions compared to the blank rolling direction $0^{\circ}, 45^{\circ}, 90^{\circ}$.

For a classical exponential hardening law, the stress of the plastic flow is defined by the following Hollomon relationship:

$$\sigma_y = K\varepsilon_p^n. \quad (1)$$

3.2. Nakajima test

The tests were carried out using test samples made of 1.4301 austenitic stainless steel, of 1 mm thickness, using the following experimental setup – a modular deep drawing unit, with exchangeable active elements, connected to a hydraulic high pressure unit and two CCD cameras connected to GOM PC with the optical strains measurement system Aramis (Fig. 6);

Fig. 6. Nakajima test experimental configuration – hydraulic high pressure unit (left), two CCD cameras mounted above the modular deep drawing unit (centre), GOM PC with Aramis software (right).

Table 3

The determined mechanical characteristics of 1.4301

	Rolling Direction		
	0°	**45°**	**90°**
Young's Modulus E[GPa]	70488.98	66703.58	69347.89
Yield Stress $R_{p0.2}$ [MPa]	266.54	254.79	271.66
Tensile Stress R_m [MPa]	621.11	576.30	600.93
Strain hardening exponent n [-]	0.52	0.53	0.54
Strength coefficient K [MPa]	1474.90	1367.57	1432.53

Table 4

The determined plane anisotropy coefficients of 1.4301

Rolling Direction	**Anisotropy coefficient r**	**Normal anisotropy coefficient $\bar{r}$**	**Planar anisotropy coefficient Δr**
0°	0.815	1.051	−0.454
45°	1.278		
90°	0.834		

Forming limit curves have been determined experimentally by using several load paths of the test samples, between the uniaxial tension ($\varepsilon_1 = -2\varepsilon_2$) and the equibiaxial stretching ($\varepsilon_1 = \varepsilon_2$) see Fig. 7. This has been obtained by realizing different test specimen geometry, suggested by Hašek (Fig. 8) [12–15].

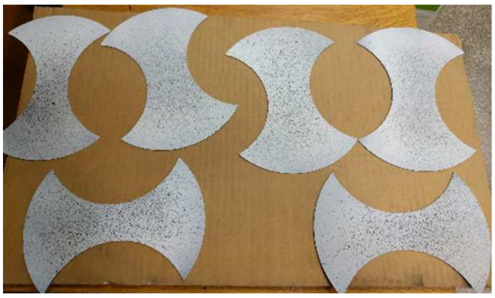

a

b

Fig. 7. Nakajima test samples with a diffuse network of points applied: *a* – before test; *b* – after test.

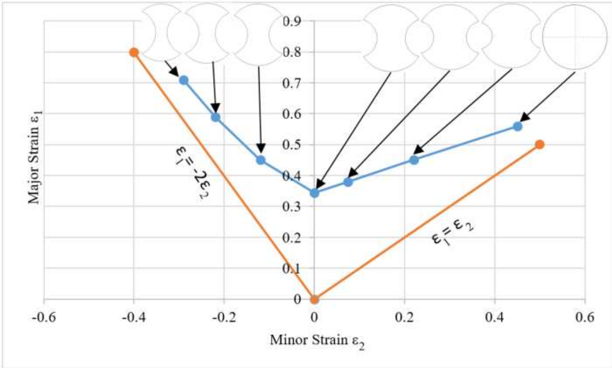

Fig. 8. Shape of the test specimens used in order to determine the FLC [13].

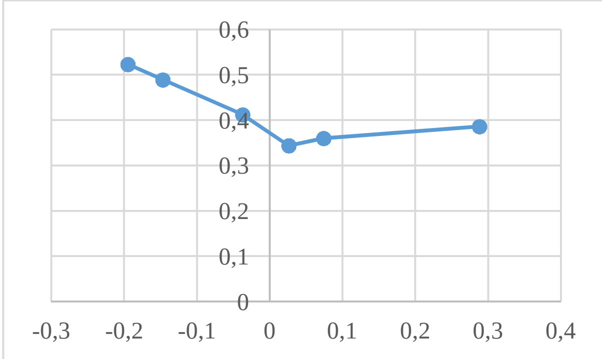

Fig. 9. Forming limit curves for 1.4301.

With the GOM setup based on a diffuse network of points applied on the test samples, it can measure their displacements during the forming process and thus it is possible to determine the forming limit curve for the test specimen. The test has been in compliance with standard ISO 12004-2:2008 and the results are represented in Fig. 9 [16].

3.3. Numerical Analysis – Finite Element Analysis

The hydroforming process has been analysed with the help of Abaqus software with the objective to determine the principal strains, material thickness and forming limits. A parametrized geometric model with finite elements was used, with only one variable R – die fillet radius (Fig. 10) [17, 18]. The 1.4301 material definition was built with the determined material properties in the previous tests. In the simulation the plastic instability criterion FLDCRT was used to help know if the material reaches it forming limits in the proposed hydroforming process.

3.4. Hydroforming Solution Development

Hydroforming experimental investigations were carried out on a turn-key hydroforming solution developed by the authors. This unique concept was built from scratch, demonstrating that the hydroforming technology can also be accessed by small research groups with knowledge in developing industrial machinery, forming technologies, hydraulics and manufacturing. The key points of the design are simple and modular design; possible exploitation for oil pressures of up to 700 bar; the possibility of manufacturing all parts in small workshops with a universal lathe machine; significant cost reduction compared to developing a deep-drawing press; the possibility of forming blanks with different thicknesses and production of various complex shapes.

Combining design knowledge with the study of hydroforming die concepts by field specialists and with the research requirements the following hydroforming solution was built, a unique hydroforming concept as seen in Fig. 11.

Sheet hydroforming (Fig. 12) involves supply of high-pressure fluid to the blank to form it into the shape of the die cavity. In the presented case the blank and die are fixed to the blank-holder pressure p_s. The forming fluid pressure p_f advances from the opposite direction and the hydroforming process takes place in three steps as presented with finite-element analysis in Fig. 13 by [19].

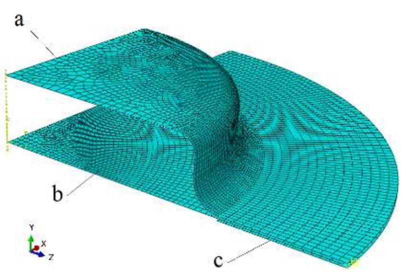

Fig. 10. FEA Abaqus – Axisymmetric assembly model for R = 6 mm: *a* – die; *b* – blank; *c* – retaining ring.

a b

Fig. 11. Unique hydroforming solutions, concept developed by the authors: *a* – CAD developed concept; *b* – Physical developed concept.

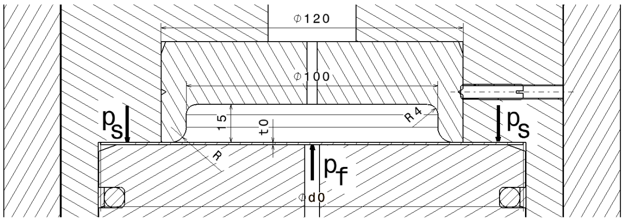

Fig. 12. Hydroforming principle schematics of the developed solution.

a b c

Fig. 13. Different stages during hydroforming of a square cup in finite-element simulation: *a* – bulging; *b* – draw-in; *c* – calibration, forming of corners [19].

3.5. Experimental measurement acquisition

The main process parameters – p_s and p_f –are monitored in real-time with a pressure transducer. In order to analyse the major and minor strains and thickness reduction, before the forming process begins the hydroforming test samples have to have electrochemically etched calibrated network of circular spots, with 1 mm diameter and 2 mm distance between centres displayed in Fig. 14. This network is recognized by a single DSLR camera connected to an external tablet (used for display and stabilization reasons) and interpreted by Argus software in order to determine the researched strain values (Fig. 15).

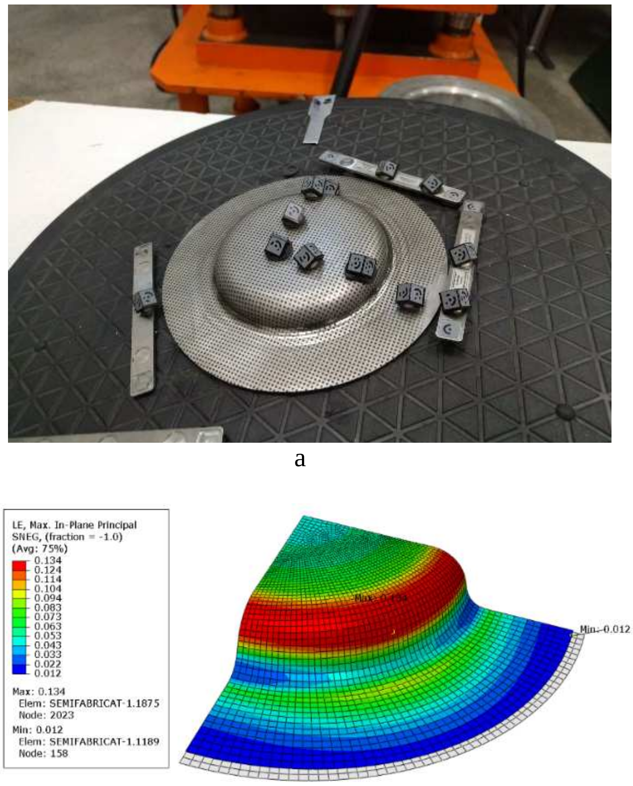

a

b

Fig. 16. Comparison between experimental and numerical drawn parts $R = 6$ mm.

Table 5

Process parameters

Symbol	Value
Blank-holder Pressure p_s [bar]	250
Forming fluid Pressure p_f [bar]	350
Initial Sheet Diameter $\emptyset d_0$ [mm]	168
Initial Sheet Thickness t_0 [mm]	1
Die Radius R [mm]	4 / 6 / 8

Fig. 15. Strain measurements on the drawn part with a DSLR camera connected to a tablet and analysed by Argus.

4. RESULTS AND DISCUSSION

The main objective of the present research was to determine and study the influence of die radius variation by hydroforming of 1.4301 austenitic stainless steel sheets. The process parameters from Table 5 are introduced in both numerical and experimental analysis to compare the main strains, thickness reduction and forming limits.

The numerical simulation results were side-by-side compared with the experimental measured results. The values are represented in Table 6.

The experimental and numerical drawn parts are represented comparatively in Fig.16.

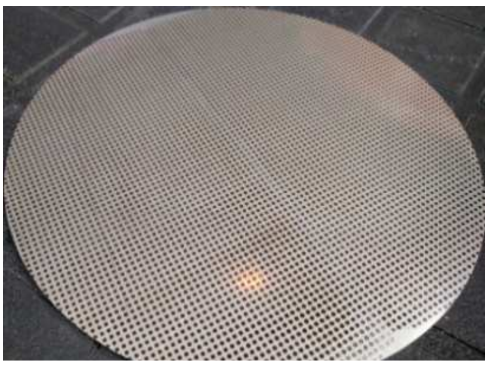

Fig. 14. Hydroforming test sample with electrochemically etched calibrated network Table 6.

Table 6

Comparison between experimental and numerical results

	Numerical simulation			Experimental measurements		
	R4	**R6**	**R8**	**R4**	**R6**	**R8**
Major Strain ε_1 [mm/mm]	0.132	0.122	0.119	0.148	0.140	0.138
Minor Strain ε_2 [mm/mm]	0.068	0.064	0.061	0.079	0.073	0.074

ACKNOWLEDGMENTS: This work was carried out with the support by Flupec Hydraulics & Pneumatics Sibiu – private company where the hydroforming press was manufactured, assembled and forming tests were carried out.

5. CONCLUSIONS

The research was based on determining many 1.4301 material characteristics to define as accurate as possible the numerical model. This model was compared to the experimental drawn parts with an own built custom solution. Despite the many error factors that can interfere with the measurements, the authors are pleased to state that the determined similar results validate the experiment methodology.

Further research can be carried out by researching variable process parameter like fluid forming pressure and blank holder pressure. This can be done be designing an experiment method with two influence factors with three variable values each.

REFERENCES

[2] J. Heizmann, *Activator Assisted Forming Technologies Status and Outlook*, in *International Conference on Hydroforming*, Fellbach, 2003.

[3] R. Vasile and O. Bologa, *Sheet Metal Hydroforming Technology – State-of-the-Art*, Applied Mechanics and Materials Vol. 841, 2016, pp. 3–9.

[4] G. Ingarao, *A sustainability point of view on sheet metal forming operations*, Journal of Cleaner Production, Vol. 29–30, 2012, p. 255–268.

[5] D. Worldwide, *2015 North American Light Vehicle Aluminum Study*, 2014.

[6] L. C. K. F. Schuster C., *Potentials and Limits with Hydroforming of Aluminium Alloys*, in Hydroforming of sheets, tubes and profiles, Fellbach, 2005.

[7] S. Gupta, R. Twardowski, P. Kucharczyk and S. Münstermann, *Experimental and Numerical Investigations of the TRIP Effect in 1.4301 Austenitic Stainless Steel Under Static Loading*, Steel research international, Vol. 85, No. 5, 2013, pp. 793–802.

[8] *Stainless steels. Technical delivery conditions for sheet/plate and strip of corrosion resisting steels for general purposes, EN 10088-2*, 2005.

[9] M. Śledź, Ł. Bąk, F. Stachowicz and W. Zielecki, *Analysis of the effect of shot peening on mechanical properties of steel sheets used as screener sieve materials*, Journal of Physics: Conference Series 451, 2013.

[10] *Metallic materials -Tensile testing - Part 1: Method of test at room temperature, ISO 6892-1*, 2009.

[11] *Metallic materials – Sheet and strip -- Determination of plastic strain ratio, ISO 10113*, 2006.

[12] J. W. Signorelli and M. d. l. A. Bertinetti, *Self-Consistent Homogenization Methods for Predicting Forming Limits of Sheet Metal*, in Metal Forming - Process, Tools, Design, InTech, 2012, pp. 175–210.

[13] D. Banabic, L. Paraianu, G. Dragos, I. Bichis and D. S. Comsa, *An improved version of the modified maximum force criterion (MMFC) used for predicting the localized necking in sheet metals*, Proceeding of the Romanian Academy, Series A, Vol. 10, No. 3, 2009.

[14] V.V. Hašek, *Berichte aus dem Institut für Umformtechnik, Universität Stuttgart* (On the stain and stress states in drawing of large un-regular sheet metal components), Essen: Giradet, 1973.

[15] C. Garjob, S. G. Racz and O. Bologa, *The Determination of the Forming Limit Curve Using a Modular Device*, Academic Journal of Manufacturing Engineering, Vol. 8, No. 2, 2010, pp. 39–44.

[16] *Metallic materials - Sheet and strip - Determination of forming-limit curves - Part 2: Determination of forming-limit curves in the laboratory, ISO 12004-2*, 2008.

[17] H. Chalal, S. G. Racz and T. Balan, *Springback of Thick Sheet AHSS Subject to Bending Under Tension*, International Journal of Mechanical Sciences, No. 59, 2012, pp. 104–114.

[18] S.G. Racz, S. Khan, H. Chalal, F. Abed-Meraim and T. Balan, *Prediction of Springback After Draw-Bending Test Using Different Material Models*, in International Conference "Advanced in Materials and Processing Technologies AMPT-2010, Paris, 2010.

[19] B. Modi and D. R. Kumar, *Development of a hydroforming setup for deep drawing of square cups with variable blank holding force technique*, No. 66, 2013, pp. 1159–1169.